

# Tunable magnetic thermal hysteresis in transition metal (Fe, Co, CoNi)/rare earth (Gd) multilayers

S. Demirtas,<sup>1</sup> M. R. Hossu,<sup>1</sup> R. E. Camley,<sup>2</sup> H. C. Mireles,<sup>3</sup> and A. R. Koymen<sup>1</sup>

<sup>1</sup>*Department of Physics, The University of Texas at Arlington, Arlington, Texas 76019, USA*

<sup>2</sup>*Department of Physics, University of Colorado at Colorado Springs, Colorado Springs, Colorado 80933, USA*

<sup>3</sup>*Physics Department, California State Polytechnic University, Pomona, California 91768, USA*

(Received 21 June 2005; published 30 November 2005)

Magnetic thermal hysteresis in Co/Gd, CoNi/Gd, and Fe/Gd multilayers is investigated by measurements of the total magnetic moment. A measurement of the magnetization as a function of temperature for the antiferromagnetically coupled multilayers displays a characteristic bow-tie shape indicating magnetic superheating and supercooling. The width of the thermal hysteresis can be tuned by an external magnetic field, with values of 150 K at fields near 100 Oe and values of 20 K near 400 Oe. The results are in good agreement with our theoretical calculations.

DOI: [10.1103/PhysRevB.72.184433](https://doi.org/10.1103/PhysRevB.72.184433)

PACS number(s): 75.60.Nt, 75.25.+z, 75.70.-i, 75.75.+a

Thermal hysteresis is an old subject, with discussions of thermal hysteresis in the phase changes of water/ice dating back to Fahrenheit and Black in the 18th century. In most cases the thermal hysteresis spans only a few degrees or less, and is strongly dependent on nucleation sites. Here we present data for a very different thermal hysteresis in a magnetic phase transition showing that thermal hysteresis (1) can occur in an entire class of magnetic multilayer systems; (2) can be exceptionally large, spanning up to 150 K; (3) can be measured by straightforward magnetization measurements and shows a distinct “bow-tie” pattern in the magnetization as a function of temperature measurements, and (4) can be dramatically tuned or eliminated by changing an external magnetic field.

We investigate multilayers composed of alternating ferromagnetic films that are antiferromagnetically coupled at the interfaces. A key feature of these multilayers is that the magnetizations of the two materials respond differently to temperature changes. For example, in the Fe/Gd multilayer<sup>1-10</sup> the average Gd magnetic moment changes from about  $7\mu_B$  to zero when the temperature is varied from 0 to around 300 K, while the moment of the Fe changes only slightly over this temperature range. We also investigate similar systems including Co/Gd (Refs. 11 and 12) and CoNi/Gd.<sup>13</sup>

The Fe/Gd system has a number of known magnetic states.<sup>1,2</sup> There is a low-temperature Gd-aligned state where the Gd magnetization is aligned with the external field (and the Fe is opposite) and there is a high-temperature Fe-aligned state where the Fe magnetization is aligned with the external field (and Gd is opposite). Finally there is also a “twisted” or canted state where the moments in each atomic layer have a different angle with respect to the applied field. This system is essentially an artificial ferrimagnet where the effective concentrations of the two magnetic components are controllable by changing the layering pattern. The phase diagram of Fe/Gd and the properties of its various phases have been the subject of considerable experimental and theoretical study.

The physical origin for the thermal hysteresis is simple. One must have two states that are stable at the same temperature. The two states are the Fe-aligned state and the Gd-

aligned state. At high temperatures, the system is typically Fe aligned, with the small Gd moments opposite to the external field. When the temperature is decreased, the Gd moments increase, but if some anisotropy holds the Fe or Gd spins in place, the system will remain in the Fe-aligned state; the net magnetic moment can even be opposite to the external field. However, if the temperature is dropped enough, this configu-

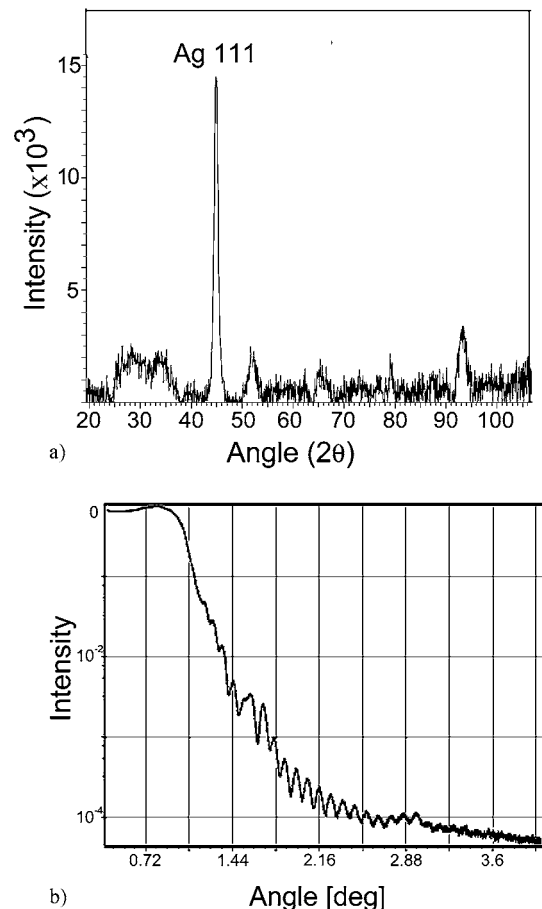


FIG. 1. (a) X-ray diffraction pattern and (b) X-ray reflectometry profile of  $(\text{Co } 4 \text{ nm}/\text{Gd } 4 \text{ nm})_8$  multilayer.

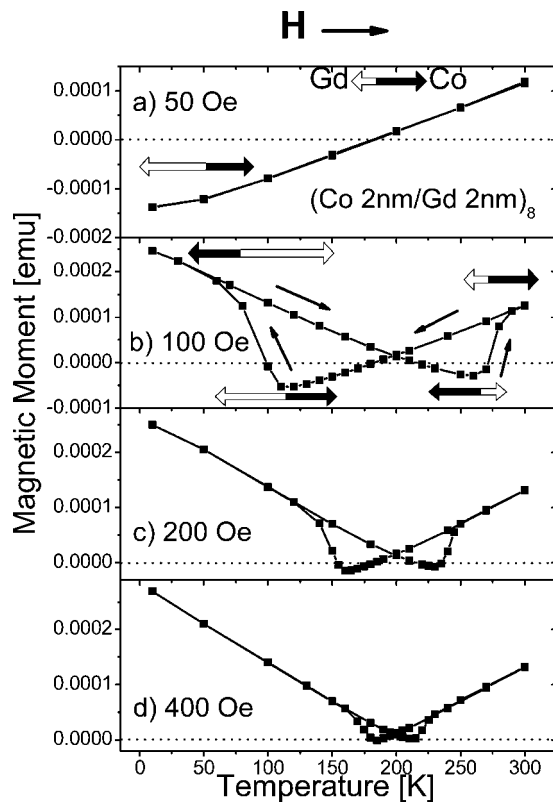


FIG. 2. Thermal hysteresis with increasing external magnetic fields for the  $(\text{Co } 2 \text{ nm}/\text{Gd } 2 \text{ nm})_8$  multilayer. The Co and Gd magnetization directions are shown as black and white arrows respectively. The external magnetic field  $\mathbf{H}$  points to the right as shown.

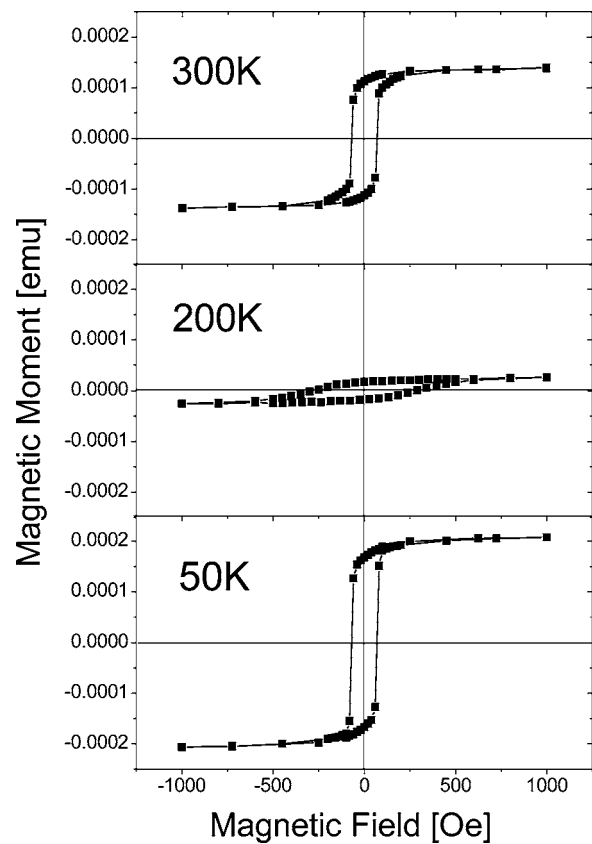


FIG. 4. Selected hysteresis loops as a function of temperature for the  $(\text{Co } 2 \text{ nm}/\text{Gd } 2 \text{ nm})_8$  multilayer.

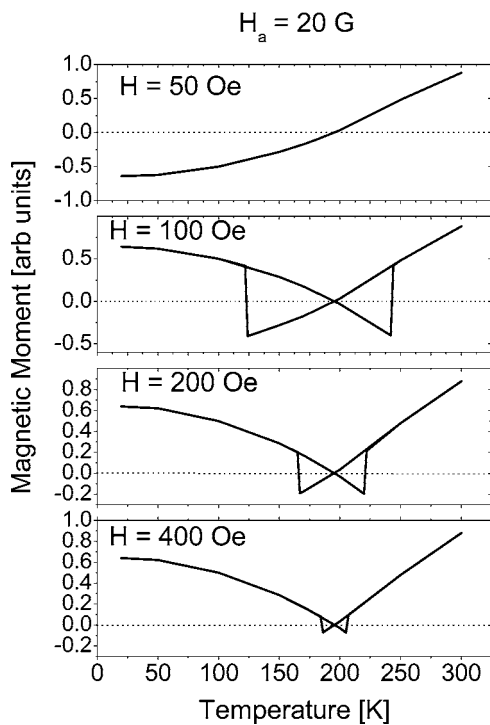


FIG. 3. Theoretical calculation for magnetization as a function of temperature for the  $(\text{Co } 2 \text{ nm}/\text{Gd } 2 \text{ nm})_8$  multilayer. A 20 Oe uniaxial anisotropy is assumed for Co in this calculation.

ration is no longer stable, and the system will reverse and have the Gd moments parallel to the applied field and the Fe moments antiparallel. A similar effect occurs on heating the system from low temperatures, except that the Gd-aligned state is held stable by anisotropy as the temperature is increased.

We note that there has recently been a theoretical discussion of thermal hysteresis<sup>14</sup> in magnetic multilayers. The theoretical calculations were done using two methods. In the first method, one minimizes Zeeman, exchange, and aniso-

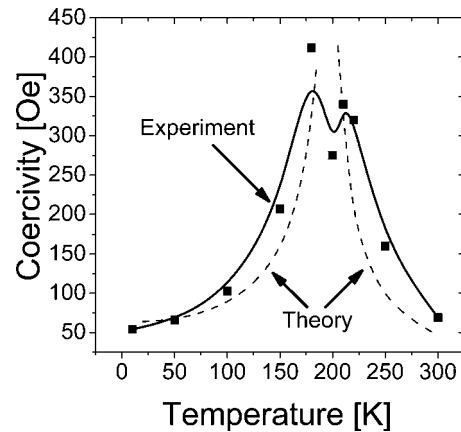


FIG. 5. Coercivity as a function of temperature for the  $(\text{Co } 2 \text{ nm}/\text{Gd } 2 \text{ nm})_8$  multilayer.

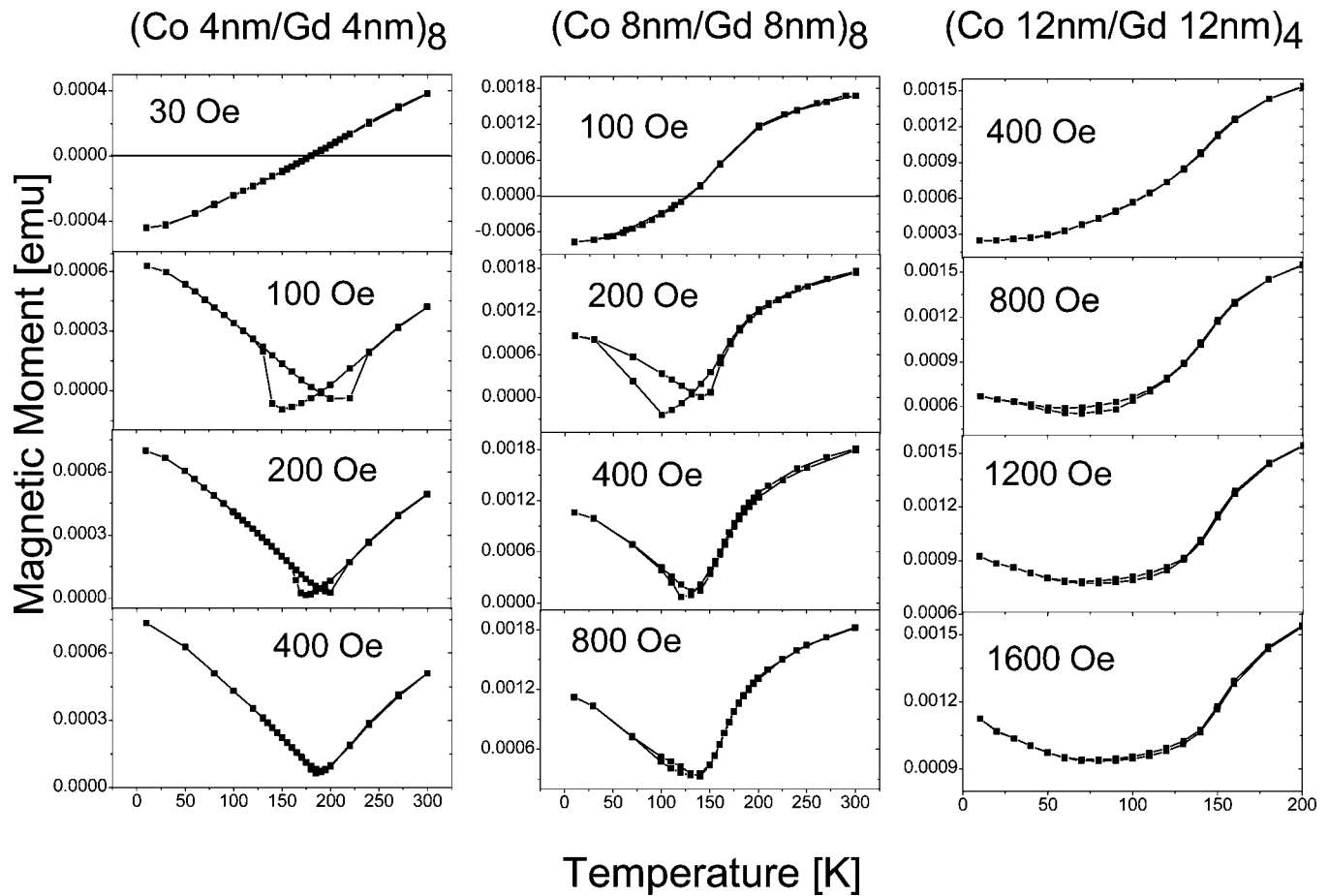


FIG. 6. Thermal hysteresis for different external magnetic fields acting on the  $(\text{Co } 4 \text{ nm}/\text{Gd } 4 \text{ nm})_8$  (left column),  $(\text{Co } 8 \text{ nm}/\text{Gd } 8 \text{ nm})_8$  (middle column), and  $(\text{Co } 12 \text{ nm}/\text{Gd } 12 \text{ nm})_4$  (right column) multilayers.

trophy energies using the assumption that each film is uniform, i.e., the magnetic moments in a given film all point rigidly locked together. In the second approach, a self-consistent local mean-field theory, one calculates the effective field on each atomic layer and treats the direction and thermal magnitude of the magnetic moment on each layer as independent variables. Similar calculations have proven to be accurate for Fe/Gd multilayers,<sup>1-4</sup> but the calculations in these earlier papers did not include anisotropy and therefore are unable to explain thermal hysteresis. We will use the self-consistent local mean-field method here, and summarize this method below.

Experimental results<sup>14</sup> have been limited to one sample and have looked only at the magnetic moment of Fe through polarized neutron scattering. There have also been related results of a first order phase transition in a similar (nonlayered) system.<sup>15</sup> The width of the thermal hysteresis in all these cases was substantially smaller (45 K or less) than that reported here. Here we present thermal hysteresis results for Co/Gd, CoNi/Gd, and Fe/Gd multilayers and show that thermal hysteresis occurs in all these systems and that it can be measured through a simple measurement of the magnetization.

Samples were prepared in a dc magnetron sputtering system at room temperature. The unbaked base pressure of the UHV deposition chamber was  $10^{-9}$  Torr. Ultrahigh-purity ar-

gon gas was used and deposition pressure was 3 mTorr. Samples were deposited on Corning glass substrates and 20-nm-thick Ag layers were used as buffer and cap layers in all samples. For the CoNi alloy, 80% is Co and 20% is Ni by weight. Deposition thicknesses were monitored *in situ* by a quartz thickness monitor calibrated by a stylus profilometer. Multilayers were deposited in various thicknesses and repetitions. Structural characterization was done using a Bruker D8 diffraction system. Magnetization measurements are taken using a superconducting quantum interference device magnetometer starting from 300 K under a constant in-plane external magnetic field (50–1600 Oe). The temperature is first reduced to 10 K and then increased back to 300 K. The temperature sweep rate was 10 K/min.

The x-ray diffraction pattern of the  $[\text{Ag } 20 \text{ nm}/(\text{Co } 4 \text{ nm}/\text{Gd } 4 \text{ nm})_8/\text{Ag } 20 \text{ nm}/\text{glass}]$  multilayer is shown in Fig. 1(a). Neither Gd nor Co has preferred orientations although the Ag has prominent [111] texture in the growth direction. Co/Gd multilayers can be considered as polycrystalline at these thicknesses. This is consistent with the isotropic in-plane angle-dependent magnetization measurements. The structural characterization of the Fe/Gd multilayers, where the thickness of the Fe and Gd layers is 4 nm, is similar to that of the Co/Gd multilayer. Thicker samples, in contrast, have preferred orientations. For a 50-nm-thick Gd layer, sandwiched between 20 nm Ag layers on top

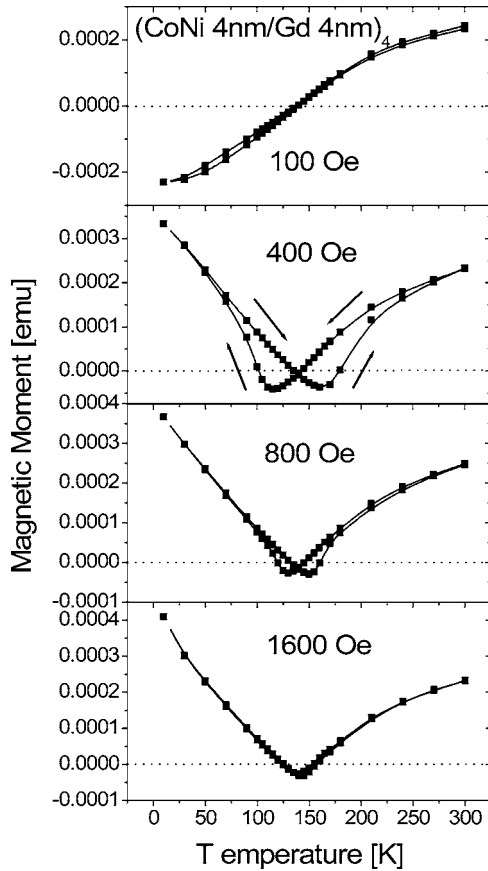


FIG. 7. Thermal hysteresis for different external magnetic fields acting on the  $(\text{CoNi } 4 \text{ nm/Gd } 4 \text{ nm})_4$  multilayer.

of glass substrate, we observed  $[10.0]$  and  $[00.2]$  textures together. The x-ray reflectivity measurement of  $[\text{Ag } 20 \text{ nm}/(\text{Co } 4 \text{ nm/Gd } 4 \text{ nm})_8/\text{Ag } 20 \text{ nm/glass}]$  multilayer is shown in Fig. 1(b). The results indicate the periodic nature of the structure and show that the system is a properly layered structure rather than a uniform alloy.

In Fig. 2, magnetization versus temperature is shown for the  $(\text{Co } 2 \text{ nm/Gd } 2 \text{ nm})_8$  multilayer for different values of the external magnetic field. In Fig. 2(a) the system is in a Co-aligned state throughout the entire temperature range. The magnetization of the Co film is initially aligned with the 50 Oe external magnetic field at 300 K. As the temperature is reduced, the thermal averaged Gd moment (unlike the Co moment) increases and becomes larger in magnitude than the Co moment and, as a result, negative magnetization is observed below 180 K. Magnetic anisotropy in the system keeps the larger Gd moment antiparallel to the external field direction even at low temperatures.

In Fig. 2(b) we see a very different behavior observed at an external field of 100 Oe. The system is originally in a Co-aligned state and remains in this state as the temperature is reduced to 110 K. Again magnetic anisotropy stabilizes the structure so that a negative magnetization is observed. Below 110 K, the structure switches from the Co-aligned to Gd-aligned configuration, exhibiting supercooling. Positive total moment is attained around 100 K and becomes more positive as the temperature is reduced. On heating from

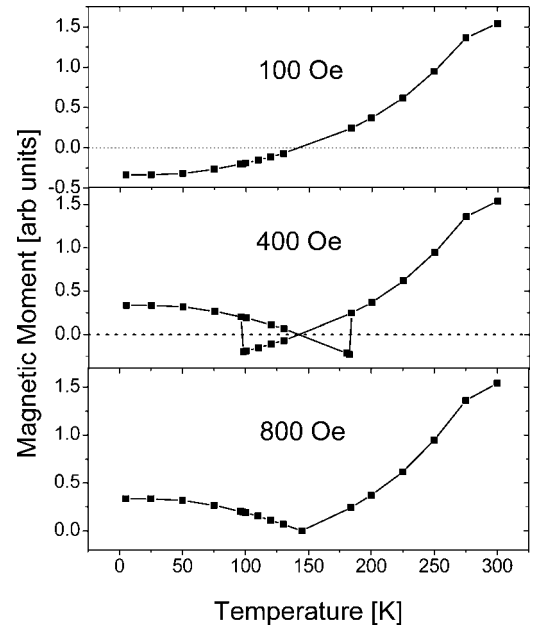


FIG. 8. Theoretical calculation for magnetization as a function of temperature for the  $(\text{CoNi } 4 \text{ nm/Gd } 4 \text{ nm})_4$  multilayer.

10 K, the Gd-aligned state is stable up to 260 K, exhibiting a negative total moment above 210 K. Above 260 K, the system switches back to its initial Co-aligned configuration, the superheating phase transition. The resulting bow-tie shape is characteristic for the thermal hysteresis and, as we will see, occurs in a number of different systems. The thermal hysteresis width, defined as the temperature interval between the minima of the bow-tie curve, spans over 150 K for 100 Oe. For 200 Oe and higher fields the width decreases as the external field increases, but retains the bow-tie shape as shown in Figs. 2(c) and 2(d).

The theoretical results for  $M(T)$  for the  $(\text{Co } 2 \text{ nm/Gd } 2 \text{ nm})_8$  structure are presented in Fig. 3. This curve is calculated for a structure with seven monolayers of Gd and 10 monolayers of Co in each unit cell. This choice of values is intended to match the experimental parameters of  $(\text{Co } 2 \text{ nm/Gd } 2 \text{ nm})$ . (We assume  $c$  axis growth for the Gd with a lattice parameter of 0.578 nm and two layers per unit cell; for Co the lattice parameter is 0.407 nm.) The spins in each monolayer are assumed to be ferromagnetically ordered and lie parallel to the film surfaces.

Only nearest neighbor exchange interactions are considered. A spin in monolayer  $i$ ,  $S_i$ , experiences a total field composed of the exchange fields from the layers above, below, and from its own layer. In addition, there are external fields and anisotropy fields:

$$H_i = J_{i,i+1}\langle S_{i+1} \rangle + J_{i,i}\langle S_i \rangle + J_{i,i-1}\langle S_{i-1} \rangle + H_z \hat{z} + H_a \langle S_i^z \rangle / S_i. \quad (1)$$

We use an anisotropy of 20 G in Co and  $H_a$  is taken to be zero in Gd. The Co moment is given as  $S_{\text{Co}}=0.86$ , a typical bulk value. The Gd moment is  $S_{\text{Gd}}=3.35$ , about 93% of its bulk value. Previous work on Fe/Gd multilayers has shown that the Gd moments are typically slightly smaller than that

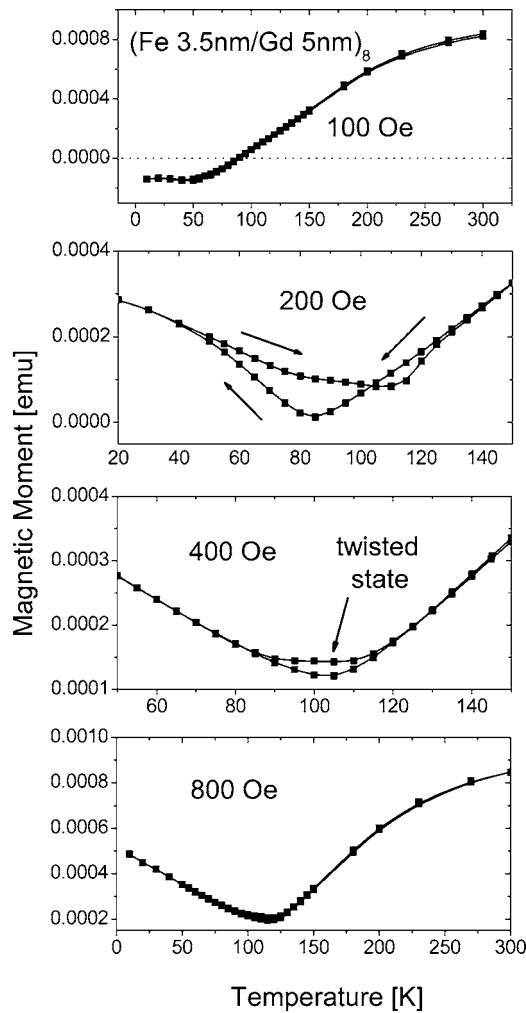


FIG. 9. Thermal hysteresis for different external magnetic fields acting on the  $(\text{Fe } 3.5 \text{ nm}/\text{Gd } 5 \text{ nm})_8$  multilayer.

found in the bulk. There are three exchange parameters. The Gd and Co exchange parameters are chosen to give the correct Curie temperature for the bulk materials— $T_c=1388 \text{ K}$  for Co and  $T_c=293 \text{ K}$  for Gd. The exchange constant for coupling between adjacent Co atomic monolayers is  $J_{\text{Co}}=6.4 \times 10^6 \text{ Oe}$ . The same value is taken for coupling between Co spins within the same atomic layer. Similarly  $J_{\text{Gd}}=1.33 \times 10^5 \text{ Oe}$  is the exchange constant for coupling between adjacent Gd atomic monolayers, and again the same value is taken for the coupling of Gd spins within a given atomic Gd layer. The interface coupling is  $J_I=-1.4 \times 10^6 \text{ Oe}$ . To take temperature into account, the thermal averaged magnitude  $\langle S_i \rangle$  is given by the Brillouin function  $\langle S_i \rangle = S_i B_S(g \mu_B S_i H_i / kT)$  where the  $g$  factor is 2;  $\mu_B$  is the Bohr magneton and  $k$  is Boltzmann's constant.

The minimum energy state is found using an iterative method where a layer of spins is chosen at random. One finds the net effective field acting on this layer and the spins in the layer are rotated to lie along this field. This lowers the energy of the system. The process is repeated until a self-consistent state is reached where the spins in each layer are aligned with the effective fields produced by the external

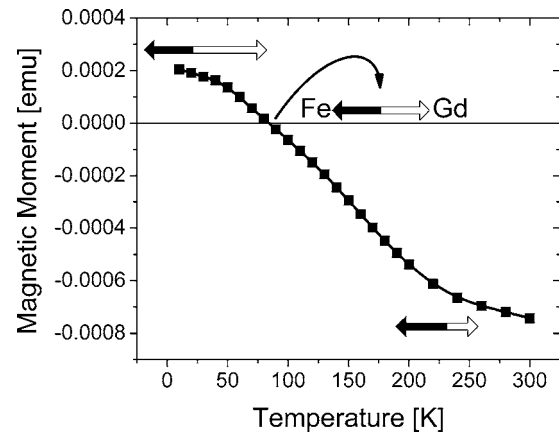


FIG. 10. Alternative measuring method of compensation temperature for  $(\text{Fe } 3.5 \text{ nm}/\text{Gd } 5 \text{ nm})_8$  multilayer.

field, the anisotropy fields and the exchange fields of the neighboring layers.

As seen in Fig. 3, the theoretical calculations are in good agreement with the experimental results. In particular, the stability of the Co-aligned phase at low fields, the bow-tie shape, and the decrease in the width of the thermal hysteresis as the applied field is increased are all reproduced by the theoretical calculations.

There can be a number of reasons for the small differences between experiment and theory. We have used a uniaxial temperature-independent anisotropy field. This is clearly just an approximation as the anisotropy is likely to be temperature dependent and also more complex than a simple uniaxial form. Furthermore, the magnetic moments may vary from layer to layer, particularly at the interfaces. Finally there is likely to be some mixing of elements at the interfaces which is not taken into account in the theory. We have attempted to use the most straightforward choice of material parameters in order to demonstrate the basic behavior, rather than carefully tailor parameter choices to fit the data.

The field-hysteresis behavior of the  $(\text{Co } 2 \text{ nm}/\text{Gd } 2 \text{ nm})_8$  multilayer is shown as a function of temperature in Fig. 4. Selected hysteresis loops are shown for three different temperatures. At low temperatures, the saturated state is the Gd-aligned state. At 200 K the system is near the compensation temperature, and at  $T=300 \text{ K}$  the Co-aligned state is the saturated state. The hysteresis loops generally appear to be square, but the width changes significantly with temperature.

The temperature-dependent coercivity is shown in Fig. 5 along with theoretical results for the same structure. As expected from rare earth/transition metal alloys, the coercivity is generally proportional to  $1/M_S$ .<sup>16,17</sup> Thus the coercivity of the hysteresis loops increases as the saturation magnetization ( $M_S$ ) decreases near compensation temperature ( $T_{\text{comp}}$ ) which explains the asymptotic maximum of the coercivity near  $T_{\text{comp}}$ . The reason for this is simple. The coercive field measures how easy it is to reverse the magnetization. The field at which this reversal takes place depends on the competition between the anisotropy energy, which would like to hold the moments in their current positions, and the Zeeman energy of the net moment in the applied field. So as the net moment decreases (near the compensation point) the aniso-

ropy energy wins out and it takes a larger field to reverse the spins. The local minimum at  $T_{\text{comp}}$  has been observed in other systems and is due to the multilayered nature of the films.<sup>8</sup> The theoretical curves are in reasonable agreement with the experimental results. This is important because it shows that a single parameter for anisotropy generates good agreement for both thermal hysteresis and field hysteresis.

The thickness dependence of the thermal hysteresis is shown in Fig. 6 for  $(\text{Co } 4 \text{ nm}/\text{Gd } 4 \text{ nm})_8$ ,  $(\text{Co } 8 \text{ nm}/\text{Gd } 8 \text{ nm})_8$ , and  $(\text{Co } 12 \text{ nm}/\text{Gd } 12 \text{ nm})_4$  multilayers. As the thickness of the films in the multilayer increases, the bow-tie shape for the thermal hysteresis distorts, but there is still some distinct thermal hysteresis. This is due to the fact that as the thickness of the individual films increases, the magnetic structure is more likely to enter twisted states near  $T_{\text{comp}}$ .<sup>18</sup> The anisotropy field cannot stabilize the magnetization in negative magnetic fields; therefore the thermal hysteresis becomes less pronounced for thicker films. Note also that for the thicker films, the thermal hysteresis generally occurs at positive magnetization values. This is consistent with our theoretical calculations which show that the magnetization does not go negative when twisted states are involved.

In Fig. 7, thermal hysteresis for the  $(\text{CoNi } 4 \text{ nm}/\text{Gd } 4 \text{ nm})_4$  multilayer is shown as a function of external magnetic field. The general features of the bow-tie shaped thermal hysteresis hold also for the thicker CoNi/Gd multilayers. For  $(\text{CoNi } 4 \text{ nm}/\text{Gd } 4 \text{ nm})_4$  multilayer, the width of the bow tie in Fig. 7 vanishes at 1600 Oe. The primary difference between the results on the CoNi/Gd sample and the earlier Co/Gd structure is that the thermal hysteresis persists in higher magnetic fields for CoNi/Gd, perhaps indicating that the effective anisotropy in the CoNi is larger than in the Co.

The calculated thermal hysteresis curves for the  $(\text{CoNi } 4 \text{ nm}/\text{Gd } 4 \text{ nm})_4$  multilayer are shown in Fig. 8. The parameters for this calculation are close to those used earlier except that  $H_a=70$  Oe in the CoNi, and the reduction factor is 0.85. As seen in Fig. 8, the theoretical calculations are in reasonable agreement with the experimental results. The compensation temperature is at 140 K, same as the experiment. Moreover, the negative magnetization at low external magnetic fields, the bow-tie shape at moderate fields, and the decrease of the thermal hysteresis width as the applied field is increased are all reproduced by theoretical calculations. The possible causes for the differences between experiment and theory have been described earlier.

In Fig. 9, thermal hysteresis for the  $(\text{Fe } 3.5 \text{ nm}/\text{Gd } 5 \text{ nm})_8$  multilayer are shown for different external magnetic fields. At low fields, the Fe-aligned state is stable over the entire temperature range, again with a negative magnetization below about 90 K. The characteristic bow-tie shaped thermal hysteresis occurs at 200 Oe. Transitions from Fe to Gd-aligned and Gd to Fe-aligned states occur respectively at 85 and 110 K. However, they take place at noticeably different positive magnetization values, therefore the shape of the bow tie is asymmetric. For 400 Oe in Fig. 9, transitions between Fe- and Gd-aligned states are through the twisted states which form the non-bow-tie thermal hysteresis. Ther-

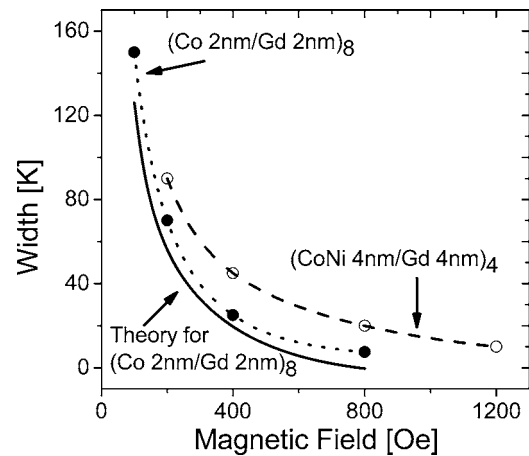


FIG. 11. Width (temperature interval between the minima) of the thermal hysteresis as a function of the external field for  $(\text{Co } 2 \text{ nm}/\text{Gd } 2 \text{ nm})_8$  and  $(\text{CoNi } 4 \text{ nm}/\text{Gd } 4 \text{ nm})_4$  multilayers. Theory for Co/Gd is shown by the solid line.

mal hysteresis vanishes at 800 Oe as shown in Fig. 9.

In thermal hysteresis measurements the midpoint of the bow tie can be considered as the conventional  $T_{\text{comp}}$ . However, the position of  $T_{\text{comp}}$  is not well defined for the multilayers that are under the effect of twisted states, i.e., the magnetization does not go to zero as is evident for the  $(\text{Fe } 3.5 \text{ nm}/\text{Gd } 5 \text{ nm})_8$  multilayer in Fig. 9 and for the  $(\text{Co } 8 \text{ nm}/\text{Gd } 8 \text{ nm})_8$  and  $(\text{Co } 12 \text{ nm}/\text{Gd } 12 \text{ nm})_4$  multilayers in Fig. 6. In Fig. 10, an alternative method for measuring  $T_{\text{comp}}$  is shown for the  $(\text{Fe } 3.5 \text{ nm}/\text{Gd } 5 \text{ nm})_8$  multilayer. The sample is first cooled under zero field to 10 K. Afterward, a high magnetic field is applied to saturate the sample into the Gd-aligned state and then the magnetic field is set to zero. The magnetic moment is then measured as a function of increasing temperature under zero field. As shown in Fig. 10,  $T_{\text{comp}}$  is 85 K for the  $(\text{Fe } 3.5 \text{ nm}/\text{Gd } 5 \text{ nm})_8$  multilayer where the total magnetization is zero. Here the anisotropy field keeps the system in the Gd-aligned configuration over the entire temperature range. Comparing with Fig. 9, the magnetization measurements at 100 Oe give a close value of 90 K.

In Fig. 11, the widths of the bow-tie curves (from dip to dip) for the  $(\text{Co } 2 \text{ nm}/\text{Gd } 2 \text{ nm})_8$  and  $(\text{CoNi } 4 \text{ nm}/\text{Gd } 4 \text{ nm})_4$  multilayers are shown as a function of external magnetic field. In addition the theoretical results for the  $(\text{Co } 2 \text{ nm}/\text{Gd } 2 \text{ nm})_8$  structure are also shown. Reasonable agreement is seen between experiment and theory. The width of a bow tie decays with increasing magnetic field.

In conclusion, the experimental results for Fe, Co, and CoNi/Gd multilayers show a significant thermal hysteresis and good agreement with the theory. The width of the thermal hysteresis can be *tuned* to have values between 0 and 150 K by moderate changes in the external magnetic field strength.

Dr. M. Lyubchenko is acknowledged for his help in structural analysis. The work at UTA was supported by The Welch Foundation Grant No. Y-1215. The work by R.E.C. was supported by the U.S. ARO Grant No. DAAD19-02-1-0174.

- <sup>1</sup>R. E. Camley and D. R. Tilley, *Phys. Rev. B* **37**, 3413 (1988).
- <sup>2</sup>R. E. Camley, *Phys. Rev. B* **39**, 12316 (1989).
- <sup>3</sup>K. Takanashi, Y. Kamiguchi, H. Fujimori, and M. Motokawa, *J. Phys. Soc. Jpn.* **61**, 3721 (1992).
- <sup>4</sup>M. Sajjeddine, Ph. Bauer, K. Cherifi, C. Dufour, G. Marchal, and R. E. Camley, *Phys. Rev. B* **49**, 8815 (1994).
- <sup>5</sup>J. G. LePage and R. E. Camley, *Phys. Rev. Lett.* **65**, 1152 (1990).
- <sup>6</sup>D. Haskel, Y. Choi, D. R. Lee, J. C. Lang, G. Srajer, J. S. Jiang, and S. D. Bader, *J. Appl. Phys.* **93**, 6507 (2003).
- <sup>7</sup>W. Hahn, M. Loewenhaupt, Y. Y. Huang, G. P. Felcher, and S. S. P. Parkin, *Phys. Rev. B* **52**, 16041 (1995).
- <sup>8</sup>S. Demirtas and A. R. Koymen, *J. Appl. Phys.* **95**, 4949 (2004).
- <sup>9</sup>S. Demirtas, A. R. Koymen, and H. Zeng, *J. Phys.: Condens. Matter* **16**, L213 (2004).
- <sup>10</sup>N. Hosoiito, H. Hashizume, and N. Ishimatsu, *J. Phys.: Condens. Matter* **14**, 5289 (2002).
- <sup>11</sup>O. S. Anilturk and A. R. Koymen, *Phys. Rev. B* **68**, 024430 (2003).
- <sup>12</sup>J. Colino, J. P. Andrés, J. M. Riveiro, J. L. Martínez, C. Prieto, and J. L. Sacedón, *Phys. Rev. B* **60**, 6678 (1999).
- <sup>13</sup>B. Altuncevahir and A. R. Koymen, *J. Magn. Magn. Mater.* **261**, 424 (2003).
- <sup>14</sup>R. E. Camley, W. Lohstroh, G. P. Felcher, N. Hosoiito, and H. Hashizume, *J. Magn. Magn. Mater.* **286**, 65 (2005).
- <sup>15</sup>C. S. Arnold, D. P. Pappas, and A. P. Popov, *Phys. Rev. Lett.* **83**, 3305 (1999).
- <sup>16</sup>P. Chaudhari, J. J. Coumo, and R. J. Gambino, *Appl. Phys. Lett.* **22**, 337 (1973).
- <sup>17</sup>D. J. Webb, A. F. Marshall, Z. Sun, T. H. Geballe, and R. M. White, *IEEE Trans. Magn.* **24**, 588 (1988).
- <sup>18</sup>B. B. Van Aken, J. L. Prieto, and N. D. Mathur, *J. Appl. Phys.* **97**, 063904 (2005).